FINAL REPORT

DEVELOPMENT OF A TWO PHOTON/LASER INDUCED FLUORESCENCE TECHNIQUE FOR THE DETECTION OF ATMOSPHERIC OH RADICALS

(NASA Grant NAG 1-818)

Submitted To:

THE NATIONAL AERONAUTICS AND SPACE ADMINISTRATION
LANGLEY RESEARCH CENTER
MAIL STOP 401A
Hampton, VA 23665

Prepared By:

Dr. John Bradshaw
School of Earth and Atmospheric Sciences
Georgia Institute of Technology
Atlanta, Ga 30332

SUMMARY

The successful development of a Two Photon/Laser Induced Fluorescence Sensor for the measurement of tropospheric OH radicals has awaited only the development of a suitable mid-Infrared(IR) laser source in the 2.9μ region. Phase I research efforts, sponsored through the National Science Foundation, evaluated numerous candidate laser systems. Of these, the only candidate system offering promise as a near term solution was the stimulated Raman shifting frequency down conversion of a commercially available Nd:YAG laser. The development of the new mid-IR laser source that was conceived at Georgia Tech was the primary goal of the Phase II NASA sponsored effort reported on here.

During phase II research efforts all of the major uncertainties that were brought out at the NASA sponsored mid-IR workshop (chaired by Dr. Crosely) have now been successfully addressed. The first stage in the frequency down conversion process has now been shown to give optimal performance using the backward stimulated Raman wave generated in Deuterium. This step has now been accomplished with > 55% photon conversion efficiency yielding > 180 mJ pulse energies in a near diffraction limited beam at an "eye safe" wavelength near 1.56μ. The second stage frequency down conversion scheme has also been demonstrated to yield output energies in excess of it's target goal of 10 mJ. The second stage system, which utilizes the stimulated backward Raman wave generated in methane, has now been shown not to require the complications of a multi-pass Raman gain cell design. A simple rugged system has now been developed that is capable of providing energies of 18 mJ/pulse in a near diffraction limited beam at 2.86μ.

Integration of this laser system into a TP-LIF OH sensor does, however, require one last engineering step, namely the construction of a liquid nitrogen cooled gas cell for the first stage deuterium Raman conversion process. Liquid nitrogen cooling of the D_2 gas is required in order to obtain a laser wavelength that will overlap an OH ro-vibronic transition. This engineering step should not be viewed as a research project, as the wavelengths of all the transitions involved are known and have been verified as part of the Phase I research effort.

The anticipated sensitivity of a TP-LIF OH sensor using this mid-IR source would give signal limited (i.e. background free) limits of detection of 1.4×10^5 OH/cm^3 under boundary layer conditions, and 5.5×10^4 OH/cm^3 under free troposphere conditions for a five minute signal integration period. This level of performance coupled with the techniques non-perturbing nature (i.e. direct measurement) and freedom from both interferences and background would allow reliable tropospheric OH measurements to be obtained under virtually any ambient condition of current interest.

1. INTRODUCTION

1.a. Overview

The hydroxyl radical (OH) is recognized as one of the pivotal species leading to the oxidation of compounds in the atmosphere. As such OH oxidative pathways lead to the removal of both naturally and anthropogenically produced substances within the troposphere such as CO, NO_2, CH_4, higher carbon number alkanes, and hydro-containing halocarbons (CFC-substitutes). Because of its importance in controlling atmospheric chemical processes, numerous instrumental techniques have been proposed for measuring the levels of atmospheric OH. However, due to its high reactivity (i.e. $OH + CH_4 \Rightarrow CH_3 + H_2O$ ($\tau \sim 1.5$ sec)) and relatively slow primary production rate (i.e. $O_3 + h\nu \Rightarrow O^1D + O_2$ ($\tau \sim 10^4 - 10^5$ sec) and $O^1D + H_2O \Rightarrow 2OH$) the steady state concentration of OH in the atmosphere is low. Model estimated levels of OH

place the concentration of this species in the part-per-quadrillion to part-per-trillion range ($10^5/cm^3$ to $10^7/cm^3$). Thus, the direct measurement of this species under atmospheric conditions has presented one of the most demanding analytical challenges yet to be undertaken by the atmospheric chemistry community.

Three "field ready" OH measurement systems were brought together in a NASA sponsored ground based and airborne intercomparison study, 1982, 1983. These three systems were: (1) the quasi-remote laser induced fluorescence (LIF) lidar method; (2) the ambient pressure LIF in-situ method; and (3) the radio-chemical $^{14}CO/CO_2$ oxidation method. The results of this intercomparison were reviewed by an independent panel, these results have been summarized by Hoell et al., and Beck et al. [2] The conclusion drawn from this review was that the only two operational systems (both single photon (SP) LIF methods) appeared to lack the sensitivity needed to routinely measure ambient OH in the clean troposphere at the $10^6/cm^3$ level with S/N ratios of 3:1 or greater within a realistically short enough measurement time.

1.b. Status of Current Techniques

More recently, several promising OH measurement techniques, which appear capable of measuring tropospheric OH, have been reported. These techniques are: the Fluorescence Assay with Gas Expansion (FAGE) low pressure LIF method of Hard and co-workers[3]; the radio-chemical $^{14}CO/^{14}CO_2$ oxidation method of Campbell and co-workers[4]; and the Ion-Assisted $^{34}SO_2/HSO_4^-$ Oxidation method of Eisele and Tanner[5,6]. The third generation FAGE instrument, which employs a 308 nm excitation/resonant fluorescence detection, has now apparently overcome the O_3/H_2O interference that was associated with early LIF techniques employing 282 nm excitation and 308 nm non-resonant fluorescence detection (i.e. $O_3 + \lambda_{282} \Rightarrow O^1D + H_2O \Rightarrow 2OH$). This third generation FAGE system has apparently eliminated the need to chemically modulate ambient OH in order to assess background levels[3,7]. The limit of detection (LOD) of this instrument for a signal to noise ratio (S/N) of 2/1 is, however, still limited to $1x10^6$ OH/cm^3 for a signal integration time of nine minutes[3]. The radio-chemical $^{14}CO/^{14}CO_2$ oxidation method ($OH + ^{14}CO \Rightarrow ^{14}CO_2$ (detected by isotopic decay)) has recently exhibited promise in identifying many of the background problems associated with earlier measurement attempts during the previously discussed OH intercomparison. Present LOD's for this technique[4] range from 1.5 to 3.0 ($x10^5$) OH/cm^3 for an ~ 2 minute sampling time and is apparently limited by background levels of $^{222}R_n$. The Ion-Assisted technique also relies on an oxidative conversion step: ($OH + ^{34}SO_2 \Rightarrow H^{34}SO_3 + O_2 \Rightarrow ^{34}SO_3 + H_2O \Rightarrow H_2{}^{34}SO_4 + NO_3^- \Rightarrow H^{34}SO_4^-$ (detected via mass spectrometry)). Although the latter approach utilizes much faster reaction (conversion) times, than the radio-chemical method (i.e. ~ 2 seconds vs. 16 seconds), and currently has an instrumental LOD of $1x10^5$ OH/cm^3 for a 5 minute signal integration period, it is apparently limited by a background[6] equivalent to $7(\pm5)x10^6$ OH/cm^3, which can be "subtracted" leaving a residual component equivalent to $4(\pm3)x10^5$ OH/cm^3.

As a point of reference[2], the single photon (SP) LIF techniques used in the 1982-1983 OH intercomparisons demonstrated LOD's of .8 to 1.5 ($x10^6$) OH/cm^3 for a signal integration time of ~ 50 minutes and background levels of < $3x10^5$ OH/cm^3.[2] In addition, representatives from the atmospheric chemistry community evaluated the OH measurement requirements necessary for testing the current understanding of OH photochemistry.[8] In the lower troposphere (1-3 km) OH can reach maximum levels of ~ $1x10^7$ OH/cm^3 under mid-day summertime conditions when UV solar flux, H_2O vapor, and O_3 are generally at their yearly maximum values. Even under these favorable conditions OH levels decrease markedly with increasing altitude dropping to ~ $1x10^6$ OH/cm^3 for mid-day conditions above 6 km. This marked change is primarily a result of the nearly three order of magnitude change in ambient water vapor

concentrations. Many significant tests of our understanding of tropospheric photochemistry, e.g. suspicion that some major reaction sequence has been omitted, can be examined using instruments capable of measuring the ambient OH concentrations of $1x10^6$ OH/cm^3 with a precision of at least 30% in a reasonable measurement time frame (i.e. < 5 min.).[8] Instrument sensitivity (LOD) in the 10^5 OH/cm^3 range is therefore required, although precise measurements at this level are not always needed.

The third generation FAGE system appears only capable of the measurement precision possible with earlier LIF instruments used in the OH intercomparison but with an ~ 6 fold improvement in temporal resolution (56 min. vs. 9 min.). The FAGE system may be limited in its ability to provide measurements which would be capable of testing photochemical theory under many conditions of interest (e.g. upper free troposphere, low UV solar flux).

Both the radio-chemical technique and the ion-assisted technique currently have similar detection capabilities that would lend themselves to investigating a wider range of atmospheric environments and conditions than afforded by the FAGE instrument. The radio-chemical technique is more limited in its measurement capabilities due to the time associated with preparative separation and analysis of the collected $^{14}CO_2$ samples with data reported to date limited to ~ 1 sample/hour, although this time scale could presumably be shortened. Neither of these techniques, however, provide a direct measurement of OH and may be more prone to a wider array of potential interferences than other more direct measurement approaches. In addition, the applicability of either technique to an airborne platform may pose non-trivial sampling problems, especially with regards to the high variability of ambient conditions found throughout the troposphere. The ion-assisted technique may offer potential advantages as a continuous automated measurement method (for at least ground based applications) once it has proven to give reliable OH measurements.

Even with the emerging techniques discussed above, there is still apparently a great need for the development of new OH measurement techniques - particularly methods that might be capable of directly measuring OH under the wide variety of atmospheric conditions that occur throughout the troposphere and that are capable of being calibrated under field sampling conditions. The two-photon LIF (TP-LIF) OH measurement scheme[9] remains a viable approach that is potentially capable of fulfilling these goals.

2 DESCRIPTION OF TECHNIQUE

2.a. TP-LIF OH Method

The measurement of ultra-trace levels of atmospheric gases via two-photon LIF and photofragmentation LIF has now proven to be a sensitive and selective method for determining the atmospherically important gases NO[10], NO_2[11], and NH_3[12]. In addition, all of these systems have now demonstrated their detection capabilities through critical instrument intercomparison [13-16]. The development of a two-photon/laser induced fluorescence for the detection of tropospheric OH, therefore, builds on what is already an extensive field proven airborne laser detection capability at Georgia Tech.

In the TP-LIF OH approach[9] depicted in figure 1, the first laser photon is used to excite OH from its ground vibrational level (v"=0) into the first vibrational level (v"=1) at an infrared wavelength, λ_1, near 2.9μ (e.g. 2Π, v"=0$\Rightarrow^2\Pi$,v"=1).

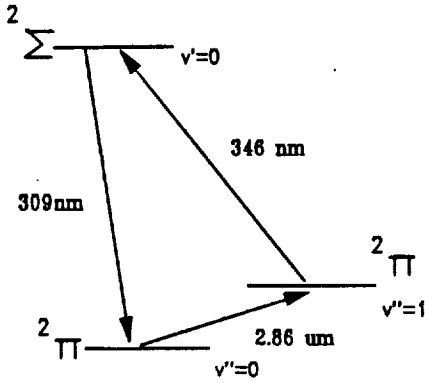

Fig. 1. Energy level diagram for TP-LIF OH Detection Scheme.

After an appropriate delay time (e.g. 10 to 20 ns.), a second laser is fired, generating a UV wavelength, λ_2, near 346 nm. The λ_2 wavelength is selected so that it corresponds to an allowed electronic transition from vibrationally excited OH to a low lying vibrational level in the first excited electronic state (e.g. $^2\Pi$, v"=1 ⇒ $^2\Sigma$, v'=0). Fluorescence can then occur at a wavelength λ_3; near 309 nm (e.g. $^2\Sigma$, v'=0 ⇒ $^2\pi$, v"=0). Like the now proven NO TP-LIF detection system, the λ_3 fluorescence wavelength is blue shifted relative to both the λ_1 and λ_2 laser excitation wavelengths. This blue shifted fluorescence presents a unique situation in that it permits virtually complete discrimination against Mie, Rayleigh, and Raman scatter of the UV probe laser. Most importantly, the nonresonant broad-band background fluorescence produced by the λ_1 and λ_2 laser beams can be reduced to near negligible levels via the use of long wavelength optical cut-off filters. Thus, the TP-LIF OH system becomes a signal limited rather than a S/N limited system as is the case for the SP-LIF OH sensor. Of even greater significance, the laser excitation wavelengths utilized in this approach eliminate the photolytic interferences that have hampered the improvement in sensitivity that could be gained by the scaling up of laser energy in single photon LIF OH techniques. In particular the interference associated with the photolysis of O_3 and subsequent $O^1D + H_2O \Rightarrow 2OH$ interference.

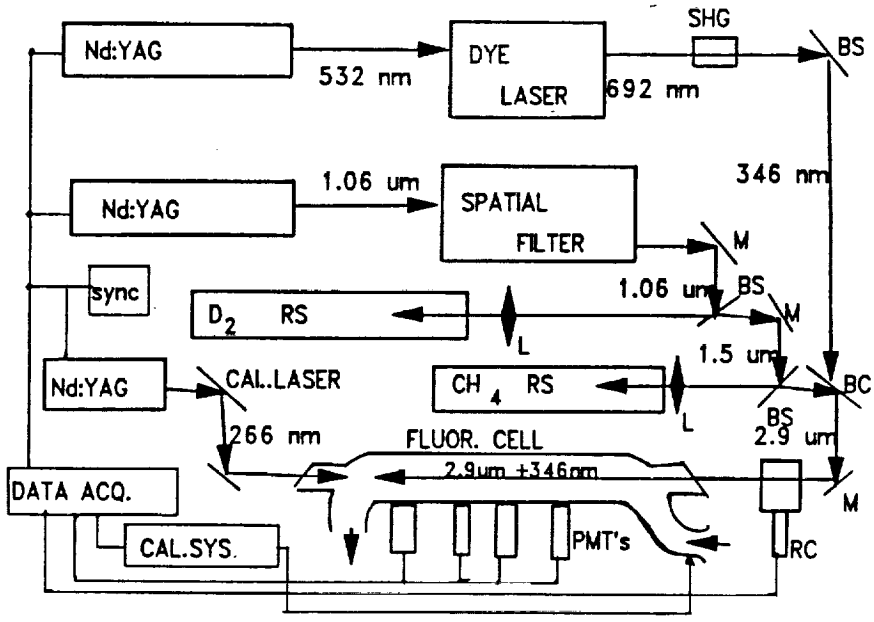

Fig. 2. TP-LIF OH instrument schematic: BC - beam combiner, BS - beam splitter, CAL. LASER - 4th harmonic Nd:YAG laser for O_3 or H_2O_2 photolysis, CAL. SYS. - standard addition O_3 or H_2O_2 for calibration, DATA ACQ. - data acquisition/control system, L - lens, M - Mirror, PMT's - photomultiplier tubes, RC - reference cell containing constant [OH] for use in data normalization, RS - Raman shifter, sync - laser synchronization and timing control.

Although the TP-LIF OH sensor (Fig. 2) may be considered a new technique, many of the hardware components will be the same as those involved in our field tested SP/LIF airborne OH instrument.[17] In addition, the characteristics required of the λ_2 UV laser (centered at ~ 346 nm), the detection optics (including custom made optical cut-off filters), and the sampling manifold needed for the TP-LIF OH system have already been developed and proven under field sampling conditions[9,17]. Similarly, most of the technology (electronics, etc.) we have developed for the TP-LIF NO instrument are directly compatible with an OH system. Finally, a calibration methodology capable of routine OH calibrations under actual ambient conditions has also been proven under field sampling conditions[17]. The only uncertainty remaining in the successful completion of the TP-LIF OH system has been the development of the suitable mid-infrared laser source that is needed for excitation of specific ro-vibronic transitions in the $^2\Pi$, v"=0 ⇒ $^2\Pi$, v"=1 manifold near 2.9μ.

Numerous pulsed mid-IR sources have been evaluated. At this time there is no commercially available system capable of generating the energy, linewidth, temporal pulse width, and low beam divergence specifications required for a sensitive TP/LIF OH sensor (i.e. $E_{\lambda 1}$ = 10 μJ, $\Delta\upsilon \leq 0.2$ cm $^{-1}$, $\Delta t < 10$ ns, $\Delta\theta < 1$ mrad, rep. rate ≥ 10 pps).

2.b. Raman Shifted Nd:YAG Laser Source

We have now developed a mid-IR laser source that is capable of meeting the target goals specified above. This source is based on the tandem D_2/CH_4 Raman shifting of a commercially available and field proven 1.06μ Nd:YAG laser.

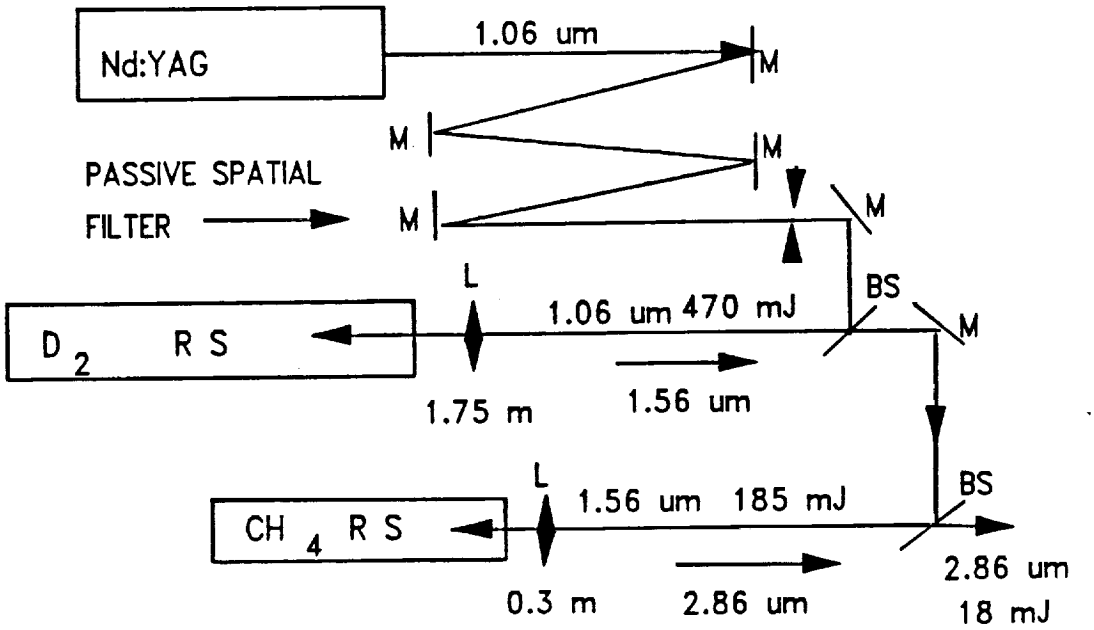

Fig. 3. Schematic represantation of tandem D_2/CH_4 Raman shifted Nd:YAG laser system: BS - beam splitter; M - Mirror; L - lens; RS - Raman Shifting gas cell.

This approach, as shown schematically in figure 3, is based on the stimulated Raman frequency conversion of the 1.06μ (9394.7cm^{-1}) Nd:YAG laser. The Q(0) first stokes Raman transition (2993.5cm^{-1}) provides the first step in this frequency conversion process generating a new laser source near 1.5μ. Tests have now shown the backward generated Raman component to be preferable to the forward generated counterpart, not only in terms of extractable first stokes energy but more importantly, in terms of the laser beam spatial characteristics, which "echo" the

pump source in the case of the backward propagating wave. The near diffraction limited output from the D_2 Raman source is then used to pump a second Raman source using the ν_1 Raman transition of CH_4 (2916.7cm^{-1}) to yield the final mid-IR laser source at 2.9μ (3484.5cm^{-1}) that will overlap the $P_1(2)$ ro-vibronic transition of OH (3484.7cm^{-1}). This second Raman laser source was again found to operate optimally using the backward propagating Raman wave. Tunability of this Raman shifted Nd:YAG laser system is obtained through temperature tuning of the Nd:YAG laser (0.9cm^{-1}/20°C).

The Nd:YAG laser used in this system is a Spectra Physics injection seeded - DCR3A having the near transform limited linewidth (< .01cm^{-1}) necessary for efficiently generating the backward propagating Raman wave (i.e. laser linewidth < Raman linewidth). Similarly, the linewidth of the D_2 Raman source (~ 0.1cm^{-1}) is sufficiently less than the CH_4 Raman linewidth (~ 0.2 cm^{-1}) to obtain reasonable energy conversion efficiency from the CH_4 Raman source. Tuning of the Nd:YAG laser (and subsequently the mid-IR frequency) by ± 0.7 cm^{-1} is easily accomplished via temperature tuning of the all solid state diode pumped Nd:YAG laser used for injection seeding.

The backward stimulated Raman conversion efficiencies were optimized following the guidelines suggested by Murray, et.al.[18]. Although CH_4 is often preferred over D_2 for generation of the forward propagating stimulated Raman component, the choice of D_2 rather than CH_4 for the first conversion step was found to be optimal for several reasons, even though CH_4 has a larger Raman cross section (i.e. higher gain). In most higher energy applications gain is of minor importance as the available pump energy density can be made large compared to the energy density required to reach threshold. The "gain difference" between these two gases merely influences the choice of pump beam focal parameters, which through the active volume influences the number density needed in the gain media (i.e. pressure), and does not effect the efficiency of the Raman conversion process (i.e. overall gain for an optimized system is approximately constant). In addition, problems associated with high energy pumping of CH_4 can also be avoided, such as: (1) carbon build up due to multi-photon photodissociation process; and (2) the need for Faraday isolators to protect the pump source from stimulated resonant backward components generated in CH_4 that do not occur in D_2.

The D_2 system was found to give optimal performance using a 1.75m focal length lens coupling the pump beam focal point approximately 1.5m into a 2m gas cell. This combination allowed for sufficiently fast enough build up of the backward component to allow efficient energy extraction while allowing the four wave mixing components in the forward direction to minimize growth of the forward propagating first stokes wave. For laser repetition rates greater than ~ 2 pps a stirred or flowing gas cell design is required. Gas circulation is required to eliminate the laser generated index of refraction gradients that otherwise deteriorate both output energy and beam quality. The CH_4 conversion step was found to give optimal performance using a 0.3m focal length lens with the 1.56μ focal point occurring ~ 0.2m into the gas cell. It is also recommended that the CH_4 cell should be of a flowing gas design above ~ 2 pps laser repetition rate.

Table I summarizes the tandem Raman laser performance characteristics obtained to date. In addition, recently acquired gradient reflective Nd:YAG resonator optics ("gaussian beam optics") have demonstrated far more usable Nd:YAG laser energy after spatially filtering (725 mJ vs. 470 mJ) than the resonator optics used to obtain the data in Table I. This higher available 1.06μ pump energy should produce a 1.5μ D_2 output energy of > 275 mJ and a 2.87μ CH_4 output energy of > 25 mJ. The Q(2) D_2 transition (2987.2cm^{-1}) was utilized in these experiments due to our current lack of a 2 m liquid nitrogen cooled Raman cell necessary for use of the Q(0) D_2 transition

($2993.5cm^{-1}$) required to obtain the final 2.9μ spectral overlap with the P(J"=2.5)1 - transition in OH.

TABLE I - Raman Laser Performance

Laser	output wavelength	linewidth	tuning range	energy/ pulse	photon conv. efficiency
Nd:YAG	1.064μ	$< 0.005cm^{-1}$	$\pm 0.7cm^{-1}$	(850mJ)	NA
DCR-OPTICS	($9394.7cm^{-1}$)			470mJ [a]	55%
Backward 1st Stokes D_2-Q(2) ($2987.2cm^{-1}$)	1.561μ ($6407.5cm^{-1}$)	$\sim 0.1cm^{-1}$	$\pm 0.7cm^{-1}$	185mJ 0.5mrad beam divergence	58% [b]
					58%
Backward 1st Stokes CH_4-ν_1 ($2916.7cm^{-1}$)	2.865μ ($3409.8cm^{-1}$)	$\sim 0.25cm^{-1}$	$\pm 0.7cm^{-1}$	18mJ 0.5mrad beam divergence	18% [c]
					10% [b]

a - spatially filtered for lowest order mode
b - conversion efficiency of spatially filtered 1.06μ pump
c - conversion efficiency of 1.5μ D_2 Raman source

3. TP-LIF OH EVALUATION OF SENSITIVITY

As presented in previous publications[9-11] the TP-LIF signal strength, $D_{\lambda 3}$, can be expressed as the product of five efficiency terms, the LIF probe volume element, and the concentration of OH radicals, namely:

$$D_{\lambda 3} = E_{\lambda 1} \times E_{\lambda 2} \times E_f \times E_d \times E_e \times V \times [OH], \quad (1)$$

where $D_{\lambda 3}$ is the number of detected signal photons per laser pulse. The efficiency terms in Eq.(1) can be further defined as follows

$E_{\lambda 1}$ = optical pumping efficiency at λ_1 (2)
$= (1-\exp(-P_{\lambda 1}\sigma_{\lambda 1}/a_{\lambda 1})xf_i$,

$E_{\lambda 2}$ = optical pumping efficiency at λ_2 (3)
$= (1-\exp(-P_{\lambda 2}\sigma_{\lambda 2}/a_{\lambda 2})xR$,

E_f = fluorescence (4)
$= k_f/(k_f + k_q[m])$,

E_d = optical detection efficiency (5)
$= \gamma_{\lambda 3} \times Y_{\lambda 3} \times Z_{\lambda 3} \times \phi_{\lambda 3}$,

E_e = electronic counting efficiency, (6)

V = volume of the sampling region (7)
$= a_{\lambda 2} \times f$ for $a_{\lambda 2} < a_{\lambda 1}$, and

$[OH]$ = concentration of OH in molecules/cm^3 . (8)

In the above equations $P_{\lambda 1}$ and $P_{\lambda 2}$ represent the number of laser photons per laser that at wavelengths λ_1 and λ_2, respectively; $\sigma_{\lambda 1}$ and $\sigma_{\lambda 2}$ are the effective absorption cross sections for OH at λ_1 and λ_2; $a_{\lambda 1}$ and $a_{\lambda 2}$ are the beam areas defined by the λ_1 and λ_2 lasers; f_i is the fraction of the total OH population in quantum state i that can be pumped a $2.9\mu m$; R is the fraction of OH initially formed in the v"=1 level that survives vibrational, rotational, spin, and parity relaxation; k_f is the reciprocal of the natural lifetime; k_q is the bimolecular electronic rate coefficient and [M] is the concentration of the quenching species.

In Eqs. (5) and (7), $\gamma_{\lambda 3}$ defines the fraction of the total fluorescence falling within the optical transmission window; $Y_{\lambda 3}$ is the optical collection collection efficiency of the f/1.4 lens system; $Z_{\lambda 3}$ is the optical filter transmission factor,

$\phi_{\lambda 3}$ is the quantum efficiency of the photomultiplier tube (PMT) at λ_3; $a_{\lambda 2}$ is again the effective beam area of the smaller of the two lasers; and f is the effective path length over which fluorescence can be monitored by a single PMT using f/1.4 lenses.

Table II. Evaluation of TP-LIF SIGNAL STRENGTH

$E_{\lambda 1}$:	$P_{\lambda 1} = 2.1\times10^{17}$ photons/pulse; $a_{\lambda 1}$=0.78 cm^{-2};	$f_i = 0.12$	$\sigma_{\lambda 1} = 3.6\times10^{-18}$ cm^2;	6.5×10^{-2}
$E_{\lambda 2}$:	$P_{\lambda 2} = 8.7\times10^{15}$ photons/pulse; $a_{\lambda 2}$=0.5 cm^2;	R=0.15	$\sigma_{\lambda 2} = 1.6\times10^{-17}$ cm^2;	3.6×10^{-2}
E_d:	$\nu_{\lambda 3} = 0.7$; $\Phi_{\lambda 3} = .23$	$Y_{\lambda 3} = 0.012$;	$Z = 0.32$;	6.2×10^{-4}
E_f:	$k_f = 1.4\times10^6$ s^{-1}; $k_q[m]_{FT} = 5.3\times10^8$	$k_q[m]_{BL} = 1.3\times10^9$ s^{-1}		1.1×10^{-3}BL 2.6×10^{-3}FT
E_e:				.9
V:	$a_{\lambda 2} = 0.5$ cm^2;	f = 1.5 cm		.75cm^3
$D_{\lambda 3}$:	$1.0\times10^{-9}\times[OH]_{BL}$ and $2.5\times10^{-9}\times[OH]_{FT}$			

Based on 15mJ at λ_1, 5 mJ at λ_2, .25cm^{-1} convoluted laser/OH overlap at both λ_1 and λ_2, BL - calculated for boundary layer (1km); FT - calculated for free troposphere (6 km).

Almost all of the terms in Equations (5-7) have been directly measured. In general, values have not changed significantly since our last assessment[9]. The only significant change involves the IR OH absorption cross-section in which recent results of Nelson et.al.[19,20] have removed most of the uncertainty associated with this term. Table II list the values of each efficiency term. The IR pumping efficiency is now estimated to be less dependent on the 2.86 μ laser energy using the revised values of the absorption cross-section (i.e. $(P_{\lambda 1}\sigma_{\lambda 1}/a_{\lambda 1}) \geq 1$)). The uncertainty associated with the $D_{\lambda 3}$ evaluation given in Table II is estimated to be less than ± a factor of 2.

The detection efficiency given in Table II reflects the observed signal counts for the detection photomultiplier tube (PMT). Scaling $D_{\lambda 3}$ to the OH probe configuration used previously having 8 PMT's with opposite sites facing back reflecting mirrors (1.5 fold gain in E_d), and 600 pulses per minute laser repetition rate, the detection efficiency for the OH system shown in Fig. (2) would be:

$D_{\lambda 3}$ Boundary Layer = 7 counts/min at 1×10^6 OH/cm^3
$D_{\lambda 3}$ Free Troposphere = 18 counts/min at 1×10^6 OH/cm^3.

For a five minute signal integration period (the maximum time anticipated using this system) at the 1×10^6 OH/cm^3 concentration range OH measurements could be made with ± 17% (1σ) precision in the boundary layer and ± 11% (1σ) in the free troposphere. The absolute magnitude of the background for this system has been shown to be < 1 count/5min under ambient sampling conditions (i.e. < 2×10^5 OH/cm^3 equivalent). Taking the minimal detectable signal to be 5 photons/integration period the signal limited detection limit of the system would be 1.4×10^5 OH/cm^3 in the boundary layer and 5.5×10^4 OH/cm^3 in the free troposphere (Fig. 4).

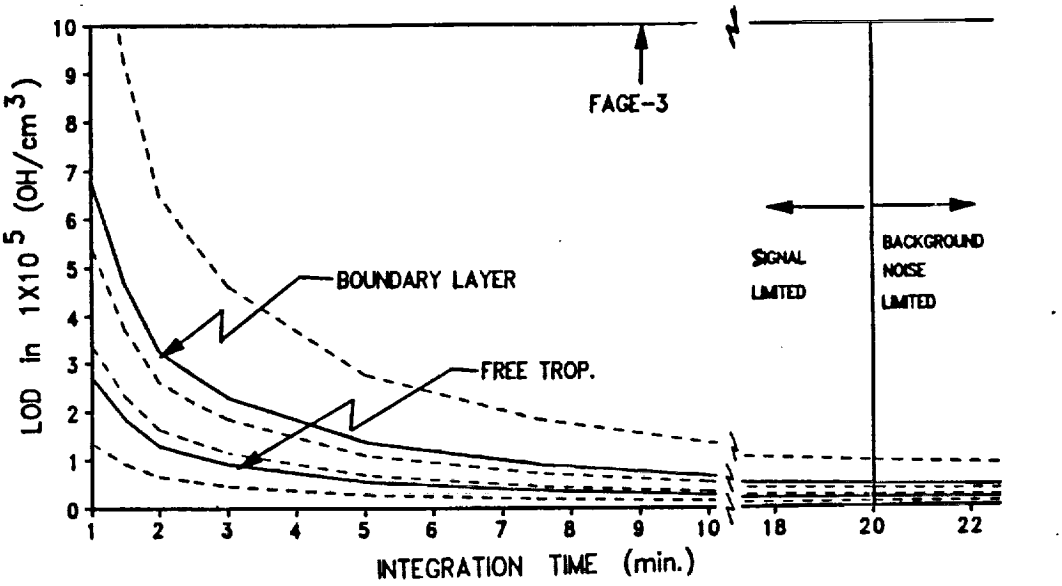

Fig. 4. TP/LIF OH estimated limit of detection (LOD) at S/N = 2/1 in units of 1x10^5 OH/cm^3 vs. signal integration time from 1 to 20 minutes. Solid line shows values derived from Table II; dashed lines depict ± factor of two uncertainty limits

4. CONCLUSIONS

Backward propagating stimulated D_2 Raman frequency down conversion of a commercially available 1.06μ Nd:YAG laser has been shown to generate an efficient source of 1.56μ radiation with near diffraction limited beam quality. Pulse energies of 180 mJ are routinely obtained. Use of guassian resonator optics in the Nd:YAG laser should yield 1.56μ energies in excess of 275mJ/pulse and may provide a useful new source for "eye-safe" LIDAR applications.

The efficient generation of a 2.9μ laser source has also been achieved using backward propagating CH_4 Raman frequency down conversion of the 1.56μ pump. A near diffraction limited beam with a pulse energy of 18mJ has now been obtained at 2.86μ and is far in excess of the system target goal of 10mJ/pulse.

Slightly higher efficiencies have also been obtained for frequency down conversion of the 1.06μ Nd:YAG using the H_2 Raman shift yielding a near diffraction limited source in the 200mJ range at 1.9μ. Similar conversion efficiencies could be anticipated as a result of extending the wavelength coverage of recently available Ti:Sapphire pulse lasers to not only cover the 740-860 nm fundamental wavelength range but also the .95 - 1.15μ and 1.06-1.33μ range using D_2 and H_2 respectively.

The anticipated sensitivity of a TP-LIF OH sensor using this mid-IR source would give signal limited (i.e. background free) limits of detection of 1.4x10^5 OH/cm^3 under boundary layer conditions and 5.5x10^4 OH/cm^3 under free troposphere sampling conditions for a five minute signal integration period. This level of performance coupled with the techniques non-perturbing nature (i.e. direct measurement) and freedom from both interferences and background would allow reliable tropospheric OH measurements to be obtained under virtually any ambient condition of current interest, including interstitial cloud sampling. Like most OH sensors, this technique could also be extended to the measurement of the peroxy radical (HO_2) through the chemical conversion process $HO_2 + NO \Rightarrow OH + NO_2$.

6. REFERENCES

1. J.M. Hoell, G.L. Gregory, M.A. Carroll, M. McFarland, B.A. Ridley, D.D. Davis, J. Bradshaw, M.O. Rodgers, A.L. Torres, G.W. Sachse, G.F. Hill, E.P. Condon, R.A. Rasmussen, M.C. Campbell, J.C. Farmer, J.C. Sheppard, C.C. Wang, L.I. Davis,

"An Intercomparison of Carbon Monoxide Nitric Oxide, and Hydroxyl Measurement Techniques: Overview of Results," Journ. Geophys. Res. 89, 11,819 - 11,825 (1984).

2. S.M. Beck, R.J. Bendura, D.S. McDougal, J.M. Hoell, Jr., G.L. Gregory, H.J. Curfman, Jr., D.D. Davis, J. Bradshaw, M.O. Rodgers, C.C. Wang, L.I. Davis, M.J. Campbell, A.L. Torres, M.A. Carroll, B.A. Ridley, G.W. Sachse, G.F. Hill, E.P. Condon, and R.A. Rasmussen, "Operational Overview of NASA GTE/CITE 1 Airborne Instrument Intercomparisons: Carbon Monoxide, Nitric Oxide, and Hydroxyl Instrumentation," Journ. Geophys. Res. 92, 1977-1985 (1987).

3. C.Y. Chan, T.M. Hard, A.A. Mehrabzadeh, L.A. George, and R.J. O'Brien, " Third-Generation FAGE Instrument for Tropospheric Hydroxyl Radical Measurement," Journ. Geophys. Res. 95, 18,569-18,576 (1990)

4. C.C. Felton, J.C. Sheppar, and M.J. Campbell, "The Radiochemical Hydroxyl Radical Measurement Method," Environ. Sci. Technol. 24, 1841-1846 (1990).

5. F.L. Eisele and D.J. Tanner, "Rapid Ion Assisted Tropospheric OH Measurements," paper presented at Fall American Geophysical Union Meeting, San Francisco (1990).

6. F.L. Eisele and D.J. Tanner, "Ion Assisted OH Measurements," Submitted to the Journ. Geophys. Res. (Oct. 1990).

7. G.P. Smith and D.R. Crosley, "A photochemical Model of Ozone Interference Effects in Laser Detection of Tropospheric OH," Journ. Geophys. Res. 95, 16,427-16,442 (1990).

8. D.R. Crosley and J.M. Hoell, "Future Directions for H_xO_y Detection," NASA Conference Publication 2448 (1986).

9. J.D. Bradshaw, M.O. Rodgers, and D.D. Davis, "Sequential two-photon laser-induced fluorescence: a new technique for detecting hydroxyl radicals," Applied Optics 23, 2134-2145(1984).

10. J.D. Bradshaw and D.D. Davis, "Sequential two-photon laser-induced fluorescence: a new method for detecting atmospheric trace levels of NO," Opt. Lett. 7, 224-226(1982).

11. S.T. Sandholm, J.D. Bradshaw, K.S. Dorris, M.O. Rodger, and D.D. Davis, "An Airborne Compatible Photofragmentation Two-Photon Laser Induced Fluorescence Instrument for Measuring Background Tropospheric Levels of NO, NO_x, and NO_2," Journ. Geophys. Res. 95, 10,155-10,162(1990).

12. J.S. Schendel, R.E. Stickel C.A. van Dijk, S.T. Sandholm, D.D. Davis and J.D. Bradshaw, "Atmospheric Ammonia measurement using a VUV/photofragmentation laser-induced fluorescence technique," Applied Optics 29, 4924-4937(1990).

13. J.M. Hoell et.al., "An Intercomparison of nitric oxide measurement techniques," Journ. Geophys. Res. 90, 12,843-12,851(1985).

14. G.L. Gregory, J.M. Hoell, Jr., A.L. Torres, M.A. Carroll, B.A. Ridley, M.O. Rodgers, J. Bradshaw, S. Sandholm, and D.D. Davis, "An Intercomparison of Airborne Nitrogen Dioxide Instruments," Journ. Geophys. Res. 95, 10,129-10,138 (1990).

15. G.L. Gregory, J.M. Hoell, Jr., M.A. Carroll, B.A. Ridley, D.D. Davis, J. Bradshaw, M.O. Rodgers, S.T. Sandholm, H.I. Schiff, D.R. Hastie, D.R. Karecki, G.I. Mackay, G.W. Harris, A.L. Torres, and A. Fried, "An Intercomparison of Airborne Nitrogen Dioxide Instruments," Journ. Geophys. Res. 95, 10,103-10,128(1990).

16. E.J. Williams, D.D. Parrish, J. Calvert, B. Watkins, M. Buhr, P.K. Quinn, R.B. Norton, S. Sandholm, J. Schendel, J. Bradshaw, A.O. Langford, P.J. Lebel, S.A. Vay, P. Roberts, and F.C. Fehsenfeld, "A Ground Based Ammonia Instrument Intercomparison," to be submitted Journ. Geophys. Res. January (1991).

17. M.O. Rodgers, J.D. Bradshaw, S.T. Sandholm, S. KeSheng, and D.D. Davis, " A 2-λ Laser-Induced Fluorescence Field Instrument for Ground-Based and Airborne Measurements of Atmospheric OH," Journ. Geophys. Res. 90, 12,819-12,834(1985).

18. J.R. Murray, J. Goldhar, D. Eimerl, and A. Szöke, "Raman Pulse Compression of Excimer Lasers For Application to Laser Fusion," IEEE Journ. of Quantum Electronics QE-15, 342-368(1979).

19. D.D. Nelson, Jr., A. Schiffman, and D.J. Nesbitt, "The dipole moment

function and vibrational transition intensities of OH," J. Chem. Phys. 90, 5455-5465 (1989).

20. D.D. Nelson, A. Schiffman, D.J. Nesbitt, "Absolute infrared transition moments for open shell diatomics from J dependence of transition intensities: Application to OH," J. Chem. Phys. 90, 5443-5454 (1989).